CrossMark

ORIGINAL PAPER

Evaluation of the depth to the bottom of magnetic sources and heat flow from high resolution aeromagnetic (HRAM) data of part of Nigeria sector of Chad Basin

T. O. Lawal[1] · L. I. Nwankwo[1]

Abstract Understanding the thermal distribution within the crust and rheology of the earth's lithosphere requires the knowledge of the Depth to the Bottom of Magnetic Sources (DBMS). This depth is an important parameter in this regard, which can be derived from aeromagnetic data and can be used as a representation for temperature at depth where heat flow values can be evaluated. In this work, high-resolution aeromagnetic (HRAM) data of part of Chad Basin (covering about 80% of the entire basin), an area bounded by eastings 769,000 and 1,049,900 mE and northings 1,200,000 and 1,500,000 mN, were divided into 25 overlapping blocks and each block was analyzed using spectral fractal analysis method. The spectral analysis method was used to obtain the Depth to the Top of Magnetic Source (DTMS), centroid depth, and DBMS. From the calculated DBMS, the geothermal gradient and heat flow parameters were evaluated and the result obtained shows that DBMS varies between 18.18 and 43.64 km. Also the geothermal gradient was found to be varying between 13.29 and 31.90 °C/km and heat flow parameters vary between 33.23 and 79.76 mW/m^2, respectively. The heat distribution of this area is one of the key parameters responsible for various geodynamic processes; therefore, this work is important for numerically understanding the thermal distribution in Chad Basin, Nigeria since rock rheologies depend on temperature, which is a function of depth.

✉ T. O. Lawal
taofeeqlawal4u@gmail.com

[1] Department of Physics, University of Ilorin, Ilorin, Nigeria

Introduction

Magnetic methods are employed for direct and indirect mapping of hydrocarbon reservoirs, geological structures, and thermal state of the crust (Glenn and Badgery 1998). The method measures variations in the magnitude of the earth's magnetic field resulting from the magnetic properties of the underlying rocks. Due to the inaccessibility and inability to cover a wide range of areas, airborne magnetic survey has been applied to acquire subsurface data in the past decades. Such data gives information about the Depth to Bottom of Magnetic Sources (DBMS), location, and extent of sedimentary basins that are required in understanding the thermal distribution in the area. Suitable information about the thermal structure of the lithosphere is necessary because of an extensive multiplicity of geodynamic examinations. These examinations include rock deformation, hydrocarbon maturation, mineral phase boundaries, rates of chemical reactions, electrical conductivity, magnetic susceptibility, seismic velocity, and mass density (Ross et al. 2006) and information about the thermal structure could only be obtained if the DBMS is known. The DBMS or Curie point depth (CPD) is the temperature at which magnetic minerals lose their ferromagnetism. Various ferromagnetic minerals have differing Curie temperatures, but the Curie temperature of titano-magnetite, the most common magnetic mineral in igneous rocks, is in the range of about 580 °C (Nwankwo et al. 2008). Magnetic minerals hotter than their Curie temperature are paramagnetic and, from the viewpoint of the earth's surface, are essentially nonmagnetic. Thus, the Curie temperature isotherm corresponds to the basal surface of magnetic crust and can be obtained from the lowest wavenumbers of magnetic anomalies, after removing the appropriate International Geomagnetic Reference Field (IGRF) from the aeromagnetic data (Ross et al. 2006). DBMS is an important parameter in understanding the temperature distribution in the crust and the rheology of the earth's lithosphere, which can be derived from

Springer

aeromagnetic data and can be used as a representation for temperature at depth (Ravat et al. 2007; Bansal et al. 2011; Nwankwo 2015).

Many studies around the world have shown that DBMS could be estimated from the analysis of aeromagnetic data; these include Okubo et al. (1985), Tanaka et al. (1999), Ross et al. (2006), Ravat et al. (2007), Bansal et al. (2011, 2013), Gabriel et al. (2011), Nwankwo et al. (2011), Kasidi and Nur (2012, 2013), Guimaraes et al. (2013), Nwankwo (2015), Nwankwo and Shehu (2015), and Abraham et al. (2015). This research work therefore presents an evaluation of DBMS, geothermal gradients, and heat flow values in part of Chad Basin, northeast Nigeria from the recently acquired high resolution aeromagnetic (HRAM) data using spectral analysis method. There are minimal records of studies on geothermal structure in Chad Basin using low resolution aeromagnetic data but no record of previous research work done using HRAM exist within the basin, though a few of them were accounted for in the upper and lower Benue trough surrounding the basin. These include Osazuwa et al. (1981) who used two profiles of gravity data in the upper Benue trough to estimate a sedimentary thickness, which is equivalent to the Depth to the Top of Magnetic Source (DTMS) varying between 1.0 and 2.2 km. Nur et al. (1999) estimated the CPD of the upper Benue trough to be varying between 23.80 and 28.70 km. Nwankwo et al. (2009) interpreted 14 well log data from an oil well in the Nigeria sector of Chad Basin and estimated the heat flow trend in the basin to be between 63.6 and 105.6 mW/m^2. Abubakar et al. (2010) also analyzed and interpreted nine aeromagnetic maps covering the upper Benue trough and obtain depth to causative body to be between 2.40 and 8.09 km. Kurowska and Schoeneich (2010) estimated the geothermal gradient values ranging from 11.37 to 58 °C/km using thermal data collected during pumping tests in water wells within the basin. Kasidi and Nur (2012) interpreted aeromagnetic data over Sarti in Northeastern Nigeria and computed CPD values varying between 26 and 28 km, geothermal gradient varying between 21 and 23 °C/km, and heat flow varying between 53 and 58 mW/m^2. Lawal et al. (2015) also obtained the DTMS over Maiduguri, northeastern part of Chad Basin to be between 1.50 and 4.20 km. Abraham et al. (2015) estimated an average DBMS in Wikki Warm Spring (WWS) located in parts of Benue Basin, which links up the Chad Basin in the north to be 10.72 km with an average thermal gradient of 54.11 °C/km and average heat flow values of 135.28 mW/m^2. An estimate of the DBMS obtained from this work would supplement the available geophysical information within the area and also contributes immensely in understanding the geothermal structures and geodynamic processes in the basin.

Location and geology of the study area

The area of study, which is a part of the sedimentary Chad Basin, Nigeria, is bounded by northings 1,200,000 and 1,500,000 mN

and eastings 769,000 and 1,049,900 mE (Fig. 1). It covers states such as Bornu, Yobe, and Jigawa. It is situated at the northwest of Northeastern Nigeria. Olugbemiro et al. (1997) reported that the Nigerian sector of Chad Basin is bounded to the east by the Mandara Mountains and in the south by the Benue trough and Biu Plateau. It encompasses the southeastern portion of the basin, which is situated in a tectonically energetic area with features, which spreads northwest to the Air Plateau and Southwest towards the Benue trough, the third and unsuccessful arm of a three-layered rift joint developed as a result of the separation of African and South American plates in early Cretaceous times (Carter et al. 1963).

Geologically, the basin, which houses the study area, has been described by many authors (Idowu and Ekweozor 1993; Nur 2001; Obaje 2009; Odebode 2010, etc.). This basin is believed to be a broad sediment-filled depression stranding Northeastern Nigeria and adjourning parts of Chad Republic. The sedimentary rocks have a cumulative thickness of over 3.6 km and consist of thick basal continental sequence and transitional calcareous deposit. It combines with the Sokoto Basin in the west of the Damergou gap between the Air and Zinder massifs (Wright et al. 1985). The generalized stratigraphic column of the Basin has been described by Odebode (2010) to be sedimentary sequence made up of Chad Formation, Kerri-Kerri Formation, Gombe Formation, Fika Shale, Gongila Formation, and Bima Sandstone. Sedimentation began in Chad (Bornu) Basin during Upper Cretaceous (probably Uppermost Albian) when over 1000 m of continental, sparsely fossil-ferrous, unwell-organized intermediate to rough-grained, feld-spathic sandstone which can be regarded to as the Bima Formation was deposited uncomfortably overlain the Precambrian basement rocks. Other sedimentary stratigraphy sequences were formed as a result of oceanic intrusion into Chad drainage and extensional deformation that occurred in the basin.

The area is marked by two distinct climatic conditions. The rainy season lasts usually from May to September with an average temperature of 30–46 °C depending on the rainfall pattern for the particular year. The dry season heralded annually by the dry, dusty Harmattan winds which blows off the Sahara Desert occurs between October and April with an average temperature of 30–37 °C. The mean annual rainfall is 7.8 mm and a relative humidity of an about 50–80%. The vegetation, which is predominantly of the Savannah-type, is divided in to two zones: Sahel Savannah towards the north and Sudan Savannah to the south.

Materials and methods

HRAM data acquisition

Thirty-two HRAM maps (sheet numbers 20, 21, 22, 23, 24, 25, 25^A, 41, 42, 43, 44, 45, 46, 47, 63, 64, 65, 66, 67, 68, 69, 70, 86, 87, 88, 89, 90, 91, 92, 112, 113, and 114) and contours of Total
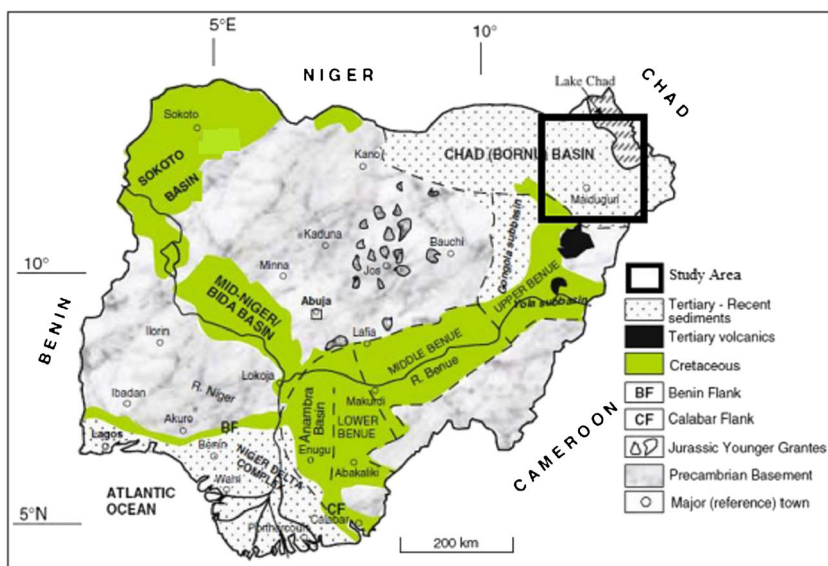
Magnetic Intensity (TMI) published by the Nigerian Geological
Survey Agency (NGSA) airborne geophysical series flown be-
tween 2004 and 2010 on a scale of 1:1000, 000 were acquired
and analyzed in this study. The acquisition, processing, and com-
pilation of the these data, which was partly financed by the
Federal Government of Nigeria and the World Bank as part of
major project known as the Sustainable Management for Mineral
Resources Project, were carried out by Fugro Airborne Surveys
Ltd. Johannesburg. The survey was acquired from an aircraft
flown at a height of 80 m with 500-m line spacing, 80-m mean
terrain clearance, and the tie line spacing of 500 m oriented in the
NW–SE direction. Regional correction based on the IGRF
(2005) was removed from the data. Reduction to the pole
(RTP) correction was performed on the data. This is because total
magnetic data contains both short and long wavelength anoma-
lies, and by applying this correction, it will correct the spatial shift
in DBMS (Li et al. 2013), the shape, and the peak of the magnetic
anomalies over their causative sources (Saada, 2016). Therefore,
RTP correction applied 0.7° declination and 1.6° inclination for
this basin using an Oasis Montaj software, version 6. Also since
DBMS is related to deep magnetic sources only and RTP mag-
netic anomalies comprise of effects of shallow and deep sources
(Thebault et al. 2010), then effects of topography and shallow
magnetic sources have to be removed from the data so that
DBMS can be accurately estimated (Saada, 2016). In view of
this, a low-pass filtering technique was adopted in this work
(Abraham et al. 2015) and an interactive filtering in the
Magmap program of Oasis Montaj software was used to remove
and boost the effects of shallow- and deep-seated magnetic
sources.

Calculating the DBMS

The application of centroid method to the aeromagnetic data is
based on the derivation of an expression by Bhattacharyya and
Leu (1977) for the power spectrum applied on the data over a
single rectangular block generalized by Spector and Grant
(1970) by assuming that the magnetic anomalies are due to
an ensemble of vertical prisms. Nwankwo (2015) and Spector
and Grant (1970) showed that the contributions from the
depth, width, and thickness of magnetic source ensembles
affect the shape of power spectrum. Therefore, Tanaka et al.
(1999) described that two methods exist in obtaining the
DBMS: the first method studied the shape of isolated magnet-
ic anomalies (Bhattacharyya and Leu 1977) while the second
examined the statistical properties of patterns of magnetic
anomalies (Spector and Grant 1970). Both methods provide
relationship between spectrum of magnetic anomalies and
depth of a magnetic source by transforming the spatial data
into frequency domain. Shuey et al. (1977) revealed that the
second method is more appropriate for regional compilations
of magnetic anomalies. Maus et al. (1997) specified that the
area required to estimate the DBMS should not be less than
few hundred kilometers.

The method used in this work for estimating DBMS is
based on the spectral analysis of magnetic anomaly data which
was described by Spector and Grant (1970). They obtained
DTMS (Z_t) and centroid depth (Z_0) from the gradient of log
power spectrum. Okubo et al. (1985) established a method in
obtaining DBMS (Z_b) based on spectral analysis of Spector
and Grant (1970). Following the technique offered by Tanaka
et al. (1999), it was assumed that the layer extends indefinitely
far in all horizontal directions. Depth to top bound of a mag-
netic source is small compared with the horizontal scale of a
magnetic source and that magnetization $M(x, y)$ is a random
function of x and y. Blakely (1995) introduced the power–
density spectra of the total field anomaly $P_{\Delta T}$:

$$P_{\Delta T}(k_x, k_y) = \Phi_M(k_x, k_y) \times F(k_x, k_y) \qquad (1)$$

Where:

$$F\left(k_x, k_y\right) = 4\pi C_m^2 |\Theta_m|^2 |\Theta_f|^2 e^{-2|k|Z_t}\left(1-e^{-|k|(Z_b-Z_t)^2}\right) \quad (2)$$

and P_M is power–density spectra of the magnetization, C_m is proportionality constant, Z_b and Z_t are basal and top depths of the magnetic source. Θ_m and Θ_f are factors for magnetization direction and geomagnetic field direction, respectively. This equation can simplified by noting that all terms are radially symmetric except $|\Theta_m|^2$ and $|\Theta_f|^2$. Also, Θ_m and Θ_f are constant. If $M(x, y)$ is totally random and uncorrelated and $P_M(k_x, k_y)$ is constant, then the radial average of $P_{\Delta T}$ can be given as:

$$P_{\Delta T}(|k|) = A_1 e^{-2|k|Z_t}\left(1-e^{-|k|(Z_b-Z_t)}\right)^2 \quad (3)$$

where A_1 is constant and k is the wavenumber. For wavelengths less than about twice the thickness of the layer, Eq. (3) can be written as:

$$\ln\left[P_{\Delta T}(|k|)^{1/2}\right] = \ln A_2 - |k|Z_t \quad (4)$$

where A_2 is a constant, and depth to the top bound of magnetic source can be obtained by fitting a straight line through the high wavenumber region of a radially average power spectrum of the magnetic anomaly.

Also, Eq. (3) can be rewritten as:

$$P_{\Delta T}(|k|)^{1/2} = A_3 e^{-|k|Z_0}\left(e^{-|k|(Z_t-Z_0)}-e^{-|k|(Z_b-Z_t)}\right) \quad (5)$$

where A_3 is a constant. At long wavelength, Eq. 5 is:

$$P_{\Delta T}(|k|)^{1/2} = A_3 e^{-|k|Z_0}\left(e^{-|k|(-d)}-e^{-|k|(d)}\right) \approx A_3 e^{-|k|Z_0} 2|k|d \quad (6)$$

where $2d$ is the thickness of the magnetic source. From Eq. 6, we can have:

$$\ln\left\{\left[P_{\Delta T}(|k|)^{1/2}\right]/|k|\right\} = \ln A_4 - |k|Z_0 \quad (7)$$

where A_4 is a constant, k is the wavenumber, and Z_0 which is the centroid of the magnetic source can be estimated by fitting a straight line through the low wavenumber region of the radially averaged frequency-scaled power spectrum. The DBMS can therefore be obtained using the relation (Okubo et al. 1985; Tanaka et al. 1999) as:

$$Z_b = 2Z_o - Z_t \quad (8)$$

Fractal-based methods of calculating the DBMS

The application of Eqs. (4) and (7) to aeromagnetic data set results in overestimation of centroid depth values due to the assumption of random and uncorrelated distribution of sources (Bansal et al. 2011; Abraham et al. 2015; Nwankwo 2015). Modifying these equations would result in scaling distribution of sources, which is equivalent to fractal distribution of magnetic sources and these modified methods are called fractal-based method of depth estimation (Bansal et al. 2011). For the fractal-based method, the radial average power spectrum of the magnetization $\phi_m(k)$ follows the relation:

$$\phi_m(k) \, \alpha \, k^{-\beta} \quad (9)$$

where β is the scaling exponent due to source distribution and its value depends on the lithology and heterogeneity of the subsurface (Bansal et al. 2011; Abraham et al. 2015). In this work, we choose 1.5 as the scaling component because the study area is a sedimentary terrain and this value is found to be appropriate (Bansal et al. 2011; Abraham et al. 2015; Nwankwo 2015). Therefore, in order to calculate the DBMS using fractal method, the power spectrum of Eqs. (4) and (9) can be combined so that the equation to be used in computing depth to the top of magnetic sources can be rewritten as:

$$\ln\left(k^{\beta}P(k)\right) = A_2 - 2kZ_t \quad (10)$$

Also, combining Eqs. (7) and (9) gives the power spectrum for computing the centroid depth and this can be rewritten as:

$$\ln\left(k^{\beta}\frac{P(k)}{k^2}\right) = A_3 - 2kZ_0 \quad (11)$$

From Eq. (8), the geothermal gradient is related to the DBMS as:

$$\frac{dT}{dZ} = \theta_c/Z_b \quad (12)$$

where θ_c is the Curie temperature approximated to be 580 °C and $\frac{dT}{dZ}$ is the geothermal gradient which could only be obtained if certain assumptions are true:

1. There are no heat sources or heat sinks between the earth's surface and the DBMS.
2. The surface temperature is 0 °C.
3. The geothermal gradient $\frac{dT}{dZ}$ is constant (Bansal et al. 2011; Nwankwo and Shehu 2015).

The heat flow q_z can also be estimated using the Fourier's equation (1955):

$$q_z = k\frac{dT}{dz} \quad (13)$$

where k is the thermal conductivity and it is assumed to be 2.5 W/m °C for igneous rocks (Bansal et al. 2011; Nwankwo 2015).

Application to HRAM data set

For the purpose of this analysis, the TMI sheets listed previously were merged in to a composite map (Fig. 2) with magnetic anomaly values ranging from −138 to 220 nT. In order to evaluate the DBMS of the study area, the composite anomaly map must be divided into blocks or lengths of various dimensions in other to obtain the basal depth. Generally, many authors have divided magnetic anomaly map into overlapping blocks ranging from 40 × 40 to 320 × 320 km and publishable results have been obtained. However, the spectrum of the map contains depth information to a length of $((L)/2\pi)$ (Shuey et al. 1997). Although if the source bodies have bases deeper than length, the spectral peak occurs at a frequency lower than the fundamental frequency for the map and cannot be resolved using spectral analysis (Abraham et al. 2015; Saada 2016). In view of the above, we first apply the spectral analysis to the RTP map with removed short wavelengths of the study

area with the dimension 277 × 385 km and give depth information about the bottom of magnetic source to be 44.10 km (Fig. 3). This depth has provided us the response of the deepest magnetic layer and has also reflected maximum spectral where the source bottom is detectable (Fig. 4). Secondly, the RTP map with short wavelengths removed was carefully overlapped (about 50% overlap) into 25 blocks covering 110 km by 110 km. The choice of the window size became necessary because of the complexity of the geology of the area and the need to sample more data point and preserve the spectral peaks (Okubo et la., 1985). In addition, Okubo et al. (1985) suggested that centroid depth estimation could be derived from data window as small as 40 × 40 km, but Ravat et al. (2007) said the window dimension of 40 × 40 km could only lead to estimates on shallow or intermediate layers and not the deepest layers. This window size was found to be appropriate for the purpose of obtaining satisfactory information about depth to the centre of magnetic source (Ravat et al.
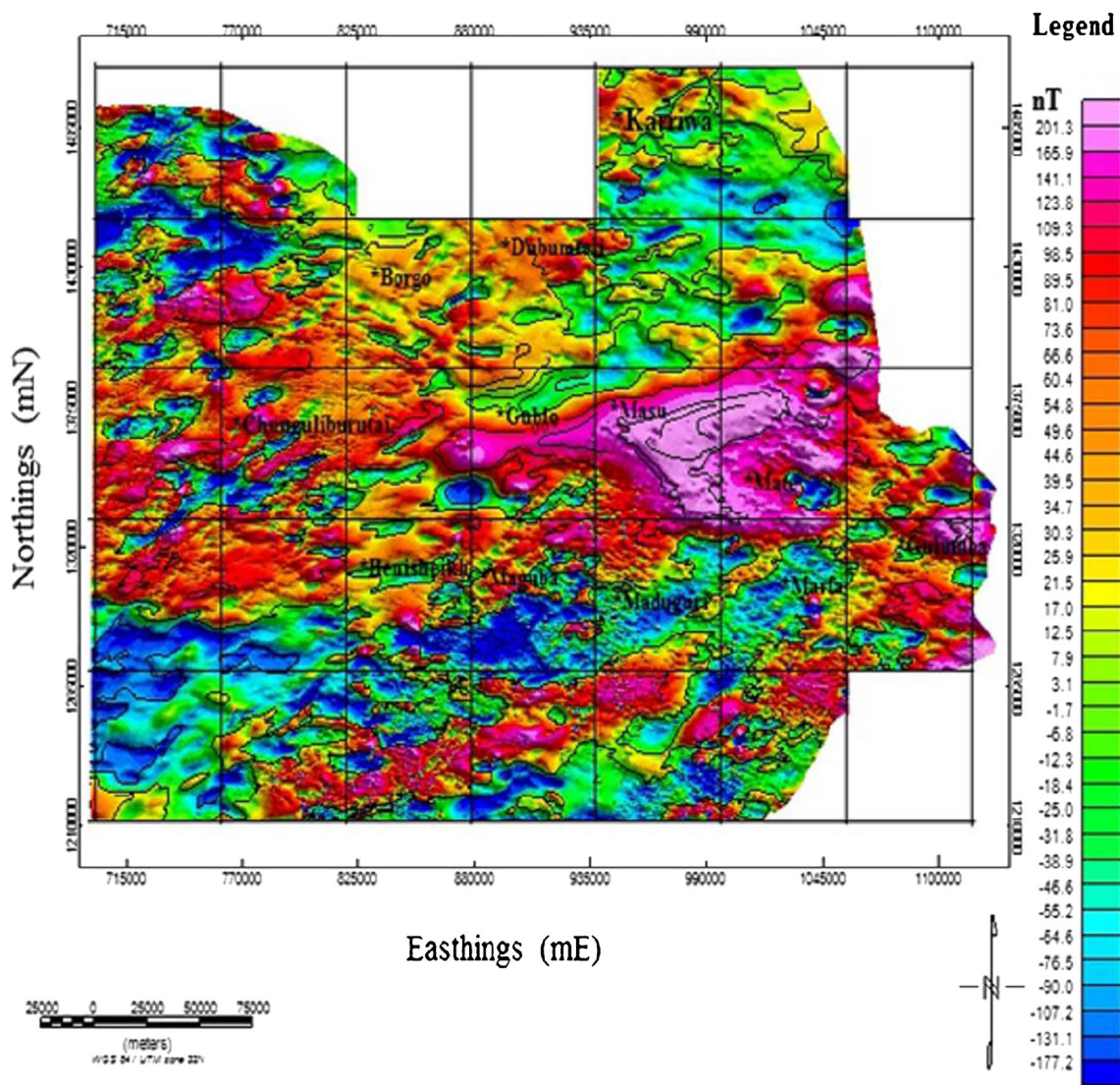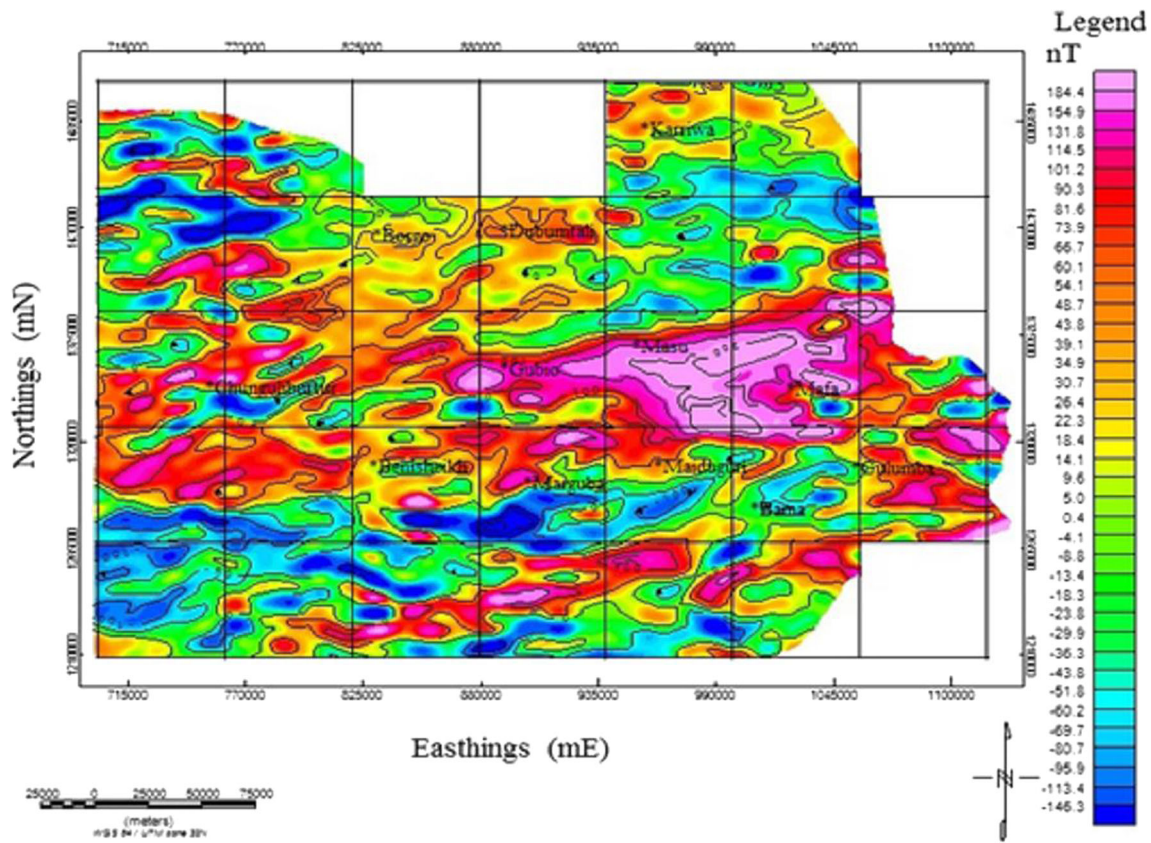

Fig. 2 Composite map of total magnetic intensity (TMI) of the study area

**Fig. 3** Reduced to pole (RTP) aeromagnetic map of the study area

2007; Nwankwo and Shehu 2015). The coordinates at the center of block which represent the sampled point were used for plotting the evaluated DBMS. The 2-D Fast Fourier Transform (FFT) was applied to each block (Eqs. 10 and 11) in order to convert the space domain grid data to the frequency domain. The DBMS (Z_b) are calculated by estimating the DTMS (Z_t) and centroid (Z_0) using (Eq. 8). The depth to the top (Z_t) and centroid (Z_0) of the magnetic source for each block were made by fitting a straight line through the high wavenumber and low wavenumber parts of the power spectrum and the scale wavenumber power spectrum, respectively. In view of the uncertainties from the slope of the straight line segment, we evaluated the standard errors from the Z_t and Z_0 using the error definition of (Ian, 2014).

However, geothermal gradient and heat flow parameters were estimated using Eqs. (12) and (13).

Results and discussion

Result of DBMS obtained from the main grid 277 × 385 window shows a value of 44.10 km where an appearance of significant spectral maximum reflects that the bottom of magnetic source is noticeable (Fig. 4) with estimated geothermal gradient of 13.15 °C/km and the evaluated heat flow of the area is 31.56 mW/m². With this result, it will be observed that the

computed geothermal gradient and the heat flow values are closer to the lower bound range values obtained from the window size of 110 × 110 km. Also, the graphical plots of natural logarithm of the power spectrum and the scaled wavenumber power spectral against wavenumber were made for each of the overlapping 12 blocks in the study area. Figure 5a shows the plot of natural logarithm of the power spectrum against wavenumber and the gradient of the high wavenumber portion leads to the estimation of the depth to the top of magnetic sources (Z_t), while Fig. 5b shows the plot of natural logarithm of the scaled wavenumber power spectral against wavenumber and the gradient of the low wavenumber portion of the plot leads to
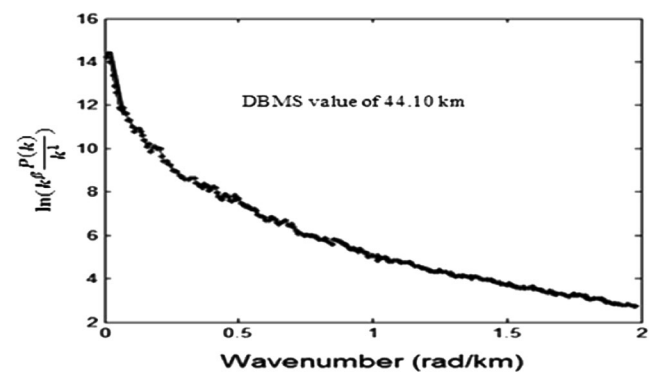
Fig. 4 Radially average power spectrum for estimation of DBMS from the main grid of the RTP TMI (277 × 385 km)
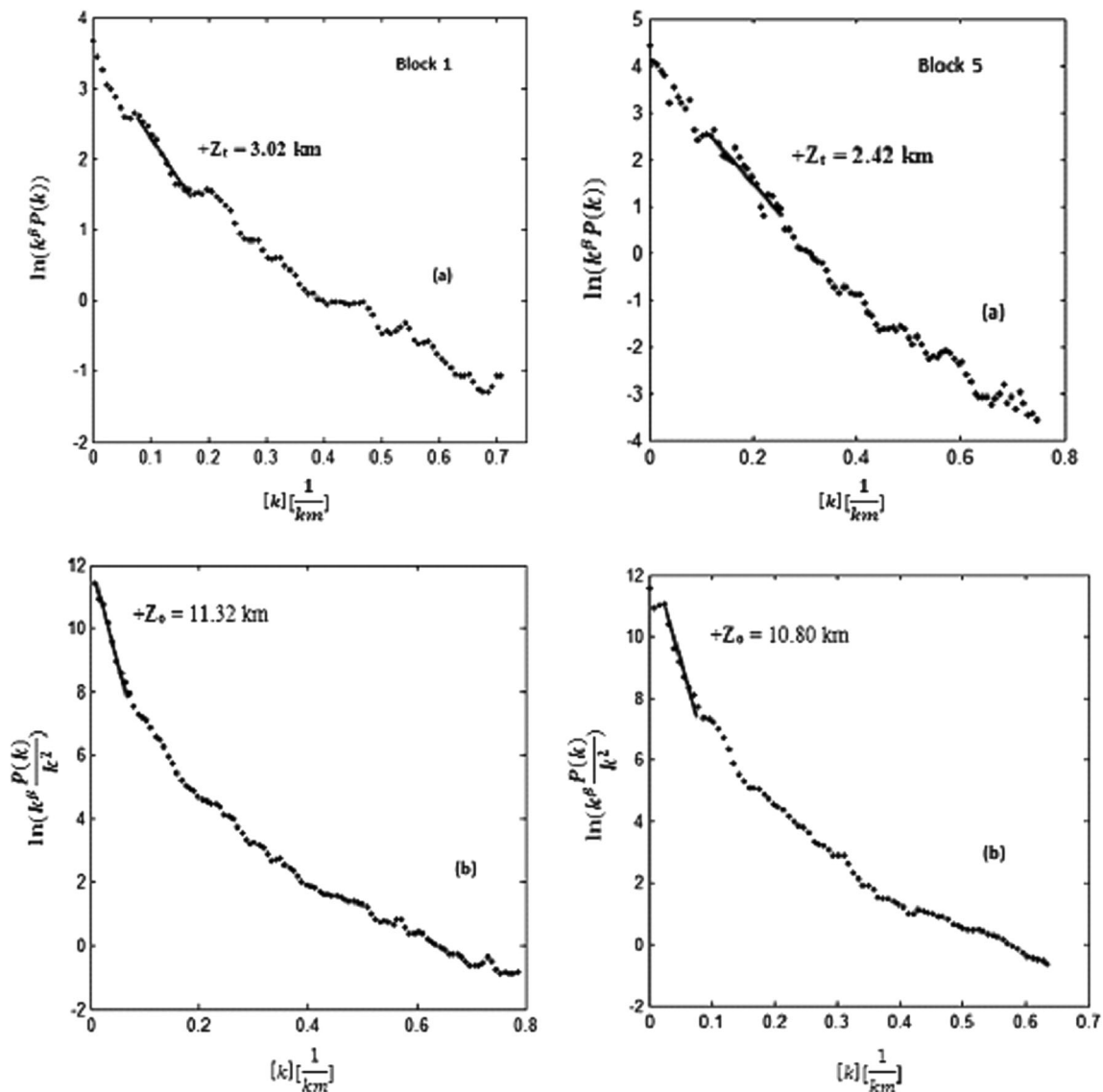
Fig. 5 Examples of radially averaged spectral plots for estimation of DTMS (**a**) and centroid depth (**b**)

the estimation of centroid method. Subsequently, the DBMS (Z_b) which is regarded as a proxy for temperature at depth was calculated using Eq. (8), while geothermal gradient and heat flow parameters were obtained using Eqs. 12 and 13. The results of the estimated depths for the 25 blocks are shown in Table 1. The DTMS ranges between 1.61 and 4.93 km with an average value of 2.93 km, the centroid depth ranges between 10.13 and 23.72 km with an average value of 15.82 km, and the DBMS values vary between 18.18 and 43.64 km with an average value of 28.70 km. In addition, the geothermal gradient was found to be varying between 13.29 and 31.90 °C/km with an average value of 21.98 °C/km and heat flow parameters vary between 33.23 and 79.76 mW/m^2 with an average value of 54.93 mW/m^2, respectively.

The variation in the depth to the top of a magnetic source obtained from the study area has revealed a spatial relationship between the elevation and depression in the Precambrian basement complex and the overlying sediments. In exploring sedimentary basins, it is a general assumption that intrusive rocks within the crystalline basement complex are truncated by erosion at their surface. With this, the depth to the top of this basement is equal to the thickness of the sediments found in the area. But Wright et al. (1985) maintain that the minimum sedimentary thickness required to attaining a threshold temperature for the beginning of hydrocarbon maturation is 2.3 km. However, results of the sedimentary thickness obtained from this study are in agreement with previous research work carried out within the basin (Nur 2001; Afolabi 2011; Lawal et al. 2015) and has a value higher than 2.3 km. Hence, hydrocarbon exploration is said to be feasible in this part of the basin. Consequently, the present research reveals that DBMS/CPD is indeed reliant on the geological situation.
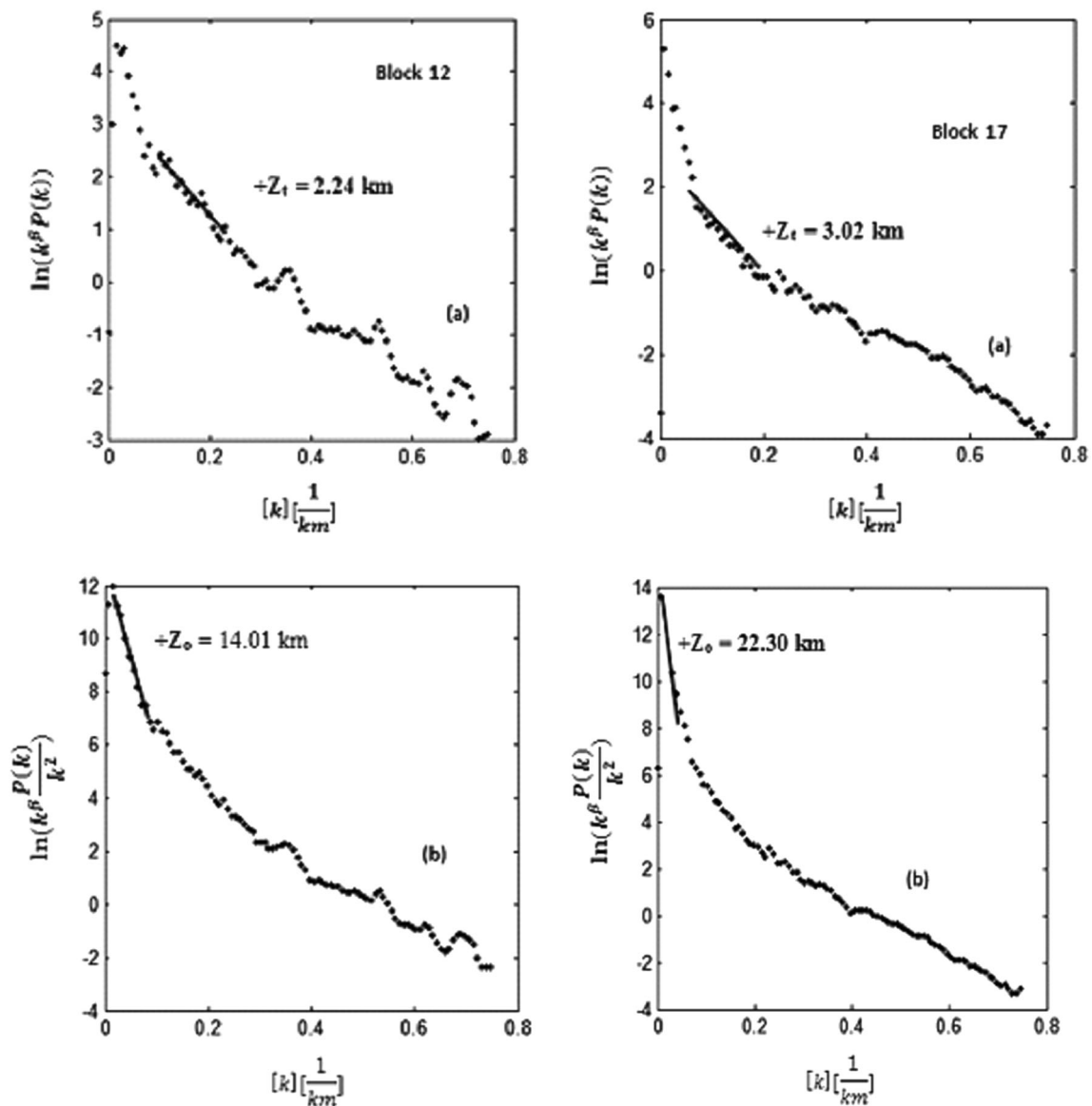
Fig. 5 continued.

Salk et al. (2005) and Nwankwo and Shehu (2015) reported that DBMS are shallower than 10 km for volcanic and geothermal fields, which are commonly associated with plate boundaries and geodynamics. However, DBMS ranging between 15 and 25 km are consequence of island arcs and ridges and deeper than 20 km in plateaus and trenches. Generally, units that comprise of high heat flow values correspond to volcanic and metamorphic regions because of high heat thermal conductivities. In addition, tectonically active regions affect the Curie depth and heat flow.

Figure 6 shows that DBMS values trend NE–SW with the shallowest (18 km) found in the northwestern portion of the basin, while deepest (> 40 km) is noticeable at the southern part of the basin. This deeper portion of the basin extends in to the Republic of Chad and Upper Benue trough where similar results have been obtained (Nur et al. 1999). They obtained a DBMS value ranging between 18 and 28 km in the Benue trough of north-central Nigeria. Also, Kasidi and Nur (2012, 2013) obtain a DBMS value ranging between 24 and 28 km in the basement complex terrain of Northeastern Nigeria. It will also be observed from the map that shallow DBMS are derivation of negative magnetization, which is found to be consistent with the low magnetic values of HRAM map (Fig. 2) and this is known fact that shallow CPD create negative magnetization (Salk et al. 2005). Generally, shallow DBMS values obtained from the study area, which corresponds to high heat flow values emphasizes the effects of large-scale tectonic event as a major influence on thermal history. Bansal et al. (2011) reported that potential regions for geothermal exploration are characterized by
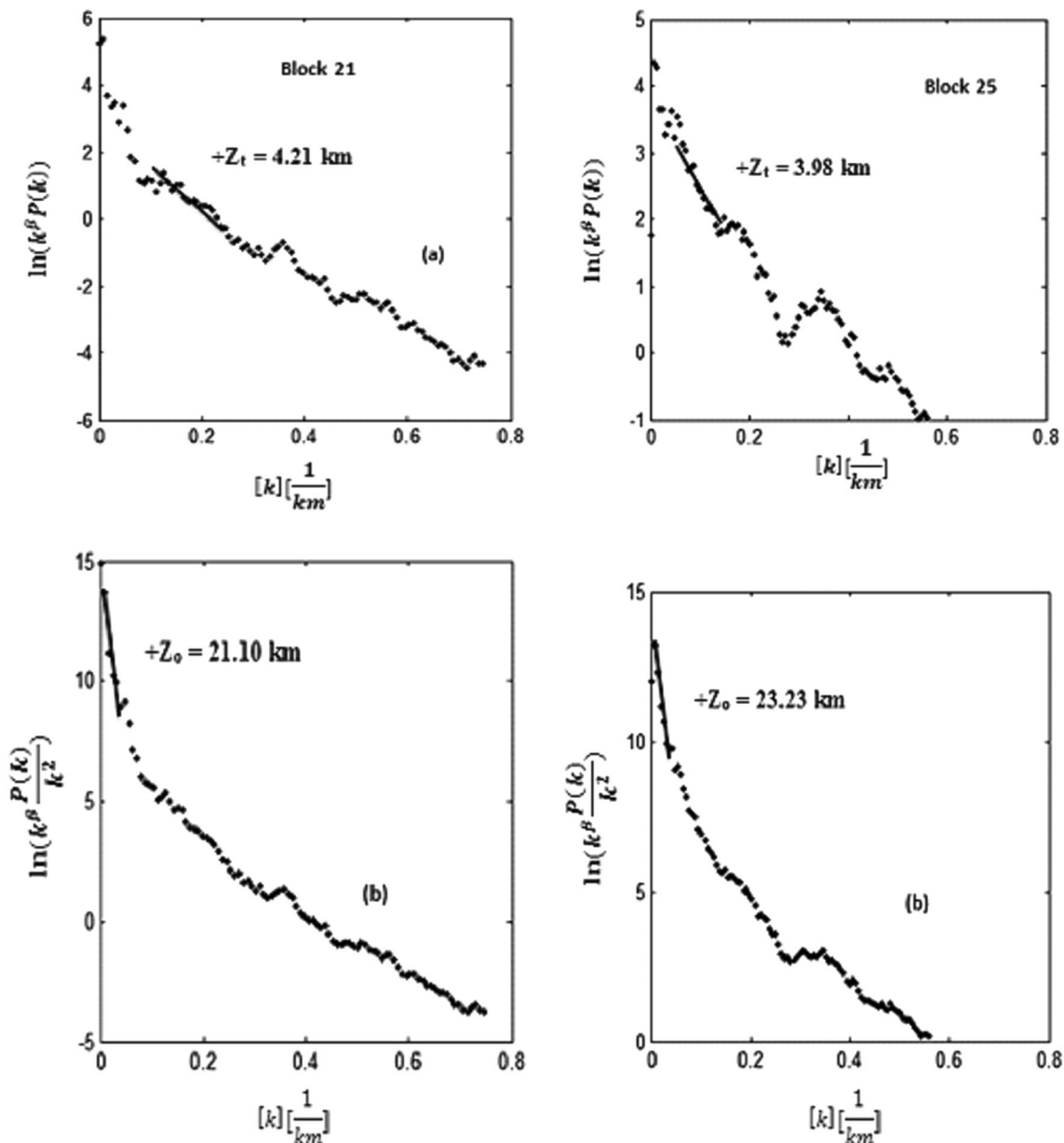
Fig. 5 continued.

high heat flow, high temperature gradient, and shallow DBMS.

Figure 7 shows the heat flow map of the study area with high heat flow observed at the northwestern portion of the area (> 72 mW/m^2) which correspond to high geothermal gradient (31.90 °C/km) and shallow DBMS (18.83 km) while low heat flow is observed at the central portion of the study area, which also correspond to low geothermal gradient and high DBMS. Nwankwo and Shehu (2015) reported that the minimum heat flow required for considerable generation of geothermal energy is close to 60 mW/m^2, while values ranging from 80 to 100 mW/m^2 and above indicate anomalous geothermal condition but these anomalous geothermal conditions were not observed in the study area. Areas observed with high flow values correspond to active volcanic and metamorphic rocks and can also be governed by deep magnetic mass that is yet to complete its cooling in association with young volcanism and faulted structures (Wright 1976). Jones (1975) also reported that regions of high geothermal gradient could lead to the generation of hydrocarbon at shallow depth, while regions of low geothermal gradient may not be viable for hydrocarbon exploration except at a greater depth. This is because geothermal gradient plays a major role in hydrocarbon generation; along with several other factors (e.g., rapid burial of organic debris in an

Table 1   Estimated heat parameters

| Blocks	Eastings (mE)	Northings (mN)	DTMS Z_t (km)	Error in Z_t	Centroid depth Z_0 (km)	Error in Z_0	DBMS Z_b (km)	Geothermal gradient (°C/km)	Heat flow (mW m^{-2})
1	770,150	1,430,150	3.02	0.035	11.32	1.250	19.62	29.56	73.90
2	770,550	1,375,400	2.86	0.043	12.60	0.048	22.34	25.96	64.91
3	770,550	1,319,450	3.24	0.032	13.25	1.322	23.26	24.94	62.34
4	770,650	1,269,150	3.35	0.042	14.50	1.388	25.65	22.61	56.53
5	770,950	1,251,550	2.42	0.026	10.80	1.872	18.18	31.90	79.76
6	825,450	1,429,750	4.93	0.012	15.57	0.641	26.21	22.13	55.32
7	823,850	1,375,800	2.74	0.054	13.80	1.210	24.86	23.33	58.33
8	825,050	1,320,650	1.61	0.016	10.24	1.521	18.87	30.74	76.84
9	825,050	1,269,050	2.09	0.018	14.25	0.865	26.41	21.96	54.90
10	825,050	1,242,050	1.76	0.054	10.13	1.488	18.50	31.35	78.38
11	880,150	1,430,150	2.28	0.052	15.00	0.785	27.72	20.92	52.31
12	879,750	1,374,650	2.24	0.043	14.01	0.241	25.78	22.50	56.25
13	880,150	1,320,250	3.32	0.038	14.59	1.112	25.86	22.43	56.07
14	880,150	1,269,800	2.12	0.041	13.32	1.351	24.52	23.65	59.14
15	877,800	1,241,650	2.32	0.032	10.78	0.324	19.24	30.15	75.36
16	934,550	1,430,550	2.42	0.037	16.90	1.126	31.38	18.48	46.21
17	934,550	1,375,450	3.24	0.042	22.30	1.821	41.36	14.02	35.06
18	934,950	1,320,650	3.61	0.021	20.50	0.694	37.39	15.51	38.78
19	934,550	1,269,800	2.71	0.032	18.96	1.421	35.21	16.47	41.18
20	934,550	1,241,400	2.43	0.026	10.80	1.521	19.17	30.26	75.64
21	989,700	1,436,600	4.21	0.043	21.10	0.821	37.99	15.27	38.17
22	989,700	1,374,250	3.80	0.026	23.72	1.321	43.64	13.29	33.23
23	988,950	1,319,850	3.20	0.031	22.63	1.231	42.06	13.79	34.47
24	990,450	1,269,550	2.33	0.028	21.10	1.432	39.87	14.55	36.37
25	1,049,250	1,320,650	3.98	0.027	23.23	1.414	42.48	13.65	34.13

oxygen-depleted environment), the right temperature needed to convert organic matters into hydrocarbon is necessary. The thermal regime in a sedimentary basin is

one of the main factors affecting the formation and accumulation of hydrocarbons. The generation of hydrocarbon and the types produced are dependent on the temperature

Fig. 6 DBMS map of the study area (CI = 1.0 km)
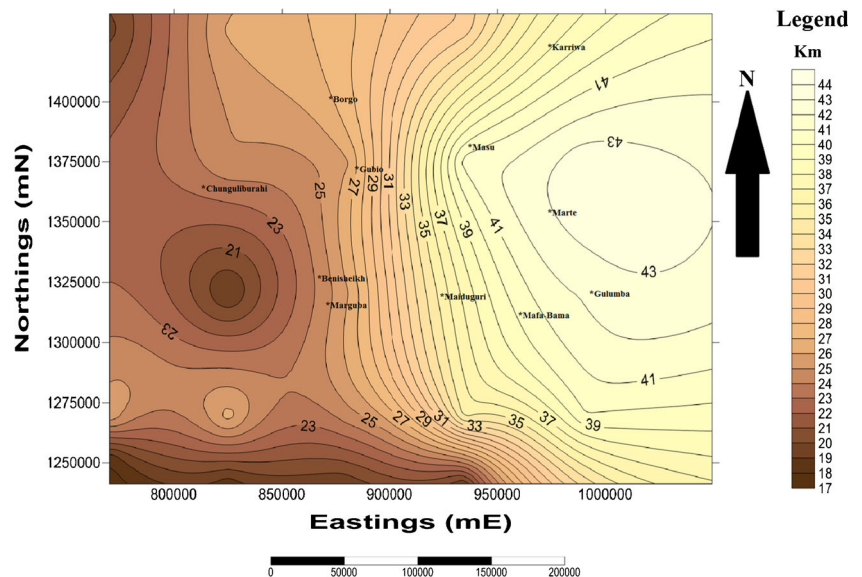
Fig. 7 Heat flow map of the study area (CI = 1.0 mW/m^2)
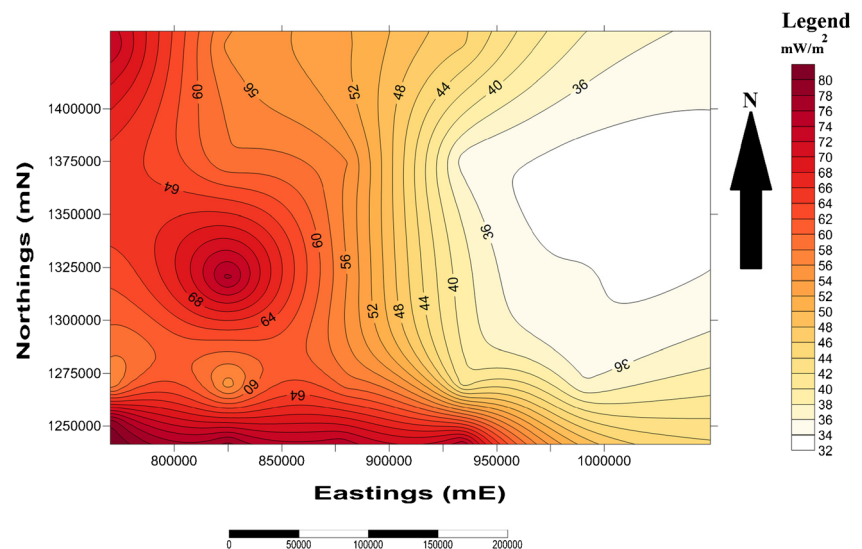
reached by the organic-rich source rocks during the burial history (Bachu and Burwash 1989). Also, since heat flow depends on the upwelling heat flow from the upper mantle where the oceanic crust is formed and more than 80% of the heat flowing to the earth's surface is from the decay of radioactive elements (K, U, and Th) in the crust and mantle but the abundance of this heat is largely hosted in the continental crust. Therefore, low values of heat flow evaluated from the southern and eastern region of the area are due to the decreasing the thickness of the continental crust to the south along the transition zone towards the oceanic portion of the African plate.

Conclusion

Evaluation of DBMS and heat flow parameters from the spectral analysis of the recently acquired TMI data of part of Nigerian sector of Chad Basin has been made. The study has therefore offered numerical information about the thermal structure, distribution, and rheology of Chad Basin, Nigeria, which can serve as a thermal index for the area. RTP and low-pass filtering technique were performed on the TMI data. The RTP is to enable the effect of true shape and position of magnetic anomalies over causative bodied to be well reflected, while low-pass filtering technique is to suppress effects from shallow magnetic sources and enhance effects from the basal ones, which are related to the Curie point depth. In view of the above, the filtered TMI data were analyzed and radially power spectrum was applied to the main grid (277 × 385 km) which gave rise to DBMS value of 44.10 km and this corresponds to the geothermal gradient of 13.15 °C/km and heat flow value of 31.56 mW/m^2. These values are very close to lower bound range obtained from the 110 × 110-km grid block size. Therefore, the DBMS values obtained from the radially average power spectrum of the 110 × 110 km grid

increase from the northwestern part of the study area to southern and eastern part of the area. The DBMS are consistent with the observed geothermal gradient and heat flow parameters. High heat flow values (> 70 mW/m^2) were observed in the northwestern part where the DBMS values are low, whereas low heat flow values (< 40 mW/m^2) were observed where DBMS values are deep. These evaluated values, which are resultant of magnetic data, show similar results with those based on well log and thermal data within the study area (Nwankwo et al. 2009; Kurowska and Schoeneich (2010). Therefore, this area is characterized by both low and high heat flow.

It would be recommended to carry out a more detailed temperature measurement located at various depths within the study area.

References

Abraham EM, Grace E, Obande M, Chukwu CG, Onwe MR (2015) Estimating depth to the bottom of magnetic sources at Wikki Warm Spring region, northeastern Nigeria, using fractal distribution of sources approach. Turkish J Earth Sci 24:494–512

Abubakar YI, Umego MN, Ojo SB (2010) Evolution of Gongola basin upper Benue Trough northeastern Nigeria. Asian J Earth Sci 3:62–72

Afolabi O, (2011) Interpretation of the gravity and magnetic data of the Chad Basin, Northeast Nigeria for hydrocarbon prospectivity. Unpub. Ph.D. thesis O.A.U. Ile-Ife

Bachu S, Burwash RA (1989) Geothermal region in the Western Canada sedimentary basin. In. Geological Atlas of the Westeran Canada Sedimentary basin. Canadian Society of petroleum Geologist and Alberta Research Council, chapt, 30

Bansal AR, Anand SP, Rajaram M, Rao VK, Dimri VP (2013) Depth to the bottom of magnetic sources (DBMS) from aeromagnetic data of Central India using modified centroid method for fractal distribution of sources. Tectonophysics 603:155–161

Bansal AR, Gabriel G, Dimri VP, Krawczyk CM (2011) Estimation of depth to the bottom of magnetic sources by a modified centroid

method for fractal distribution of sources: an application to aeromagnetic data in Germany. Geophysics 76(3):L11–L22

Bhattacharyya BK, Leu LK (1977) Spectral analysis of gravity and magnetic anomalies due to rectangular prismatic bodies. Geophysics 42:41–50

Blakely RJ (1995) Potential theory in gravity and magnetic applications. Cambridge Univ Presstime 307–308

Carter JD, Barber W, Tait EA, Jones DG, (1963) The geology of parts of Adamawa, Bauchi and Bornu Provinces in Northeast Nigeria: Bulletin, Geology Survey of Nigeria. 108

Fourier J (1955) Analytical theory of heat. Dover Publications New, York

Gabriel G, Dressel I, Vogel D, Krawczyk CM (2011) Curie depths estimation in Germany: methodological studies for derivation of geothermal proxies using new magnetic anomaly data. Geophysical Research letter 13:EGU2011–EGU6938

Glenn WE, Badgery RA (1998) High resolution aeromagnetic surveys for hydrocarbon exploration: prospect scale interpretation. Canadian J Explor Geophys 34(1&2):97–102

Guimaraes SNP, Hamza VM, Ravat D (2013) Curie depths using combined analysis of centroid and matched filtering methods in inferring thermomagnetic characteristics of central Brazil. 13th International Congress of the Brazilian Geophysical Society, Rio de Janeiro, Brazil 26–29

Idowu JA, Ekweozor CM (1993) Petroleum geochemistry of some upper cretaceous shale from upper Benue trough and south western Chad Basin, Nigeria. J Min Geol 25:131–149

Ian C (2014) Doing physics with MATLAB. University of Sydney, School of Physics

Jones PH (1975) Geothermal and hydrocarbon regimes, Northern Gulf of Mexico Basin: Proceedings of the first Geo pressured Geothermal Energy Conference. Louisiana State University, Baton Rouge

Kasidi S, Nur A (2012) Curie depth isotherm deducted from spectral analysis of magnetic data over Sarti and environs North-eastern Nigeria. Int. J Earth Sci 5:1284–1290

Kasidi S, Nur A (2013) Spectral analysis of magnetic data over Jalingo and environs north-eastern Nigeria. Int J Sci Res 2:447–454

Kurowska E, Schoeneich K, (2010) Geothermal exploration in Nigeria. In: Proceedings of the world geothermal congress; Bali, Indonesia. 25–29

Lawal TO, Nwankwo LI, Akoshile CO (2015) Wavelet analysis of aeromagnetic data of Chad Basin, Nigeria. African Rev Phys 10:111–120

Li CF, Wang J, Lin J, Wang T (2013) Thermal evolution of the North Atlantic lithosphere: new constraints from magnetic anomaly inversion with a fractal magnetization model. Geochem Geophys Geosyst 14:5078–5105

Maus S, Gordon D, Fairhead D (1997) Curie temperature depth estimation using a self-similar magnetization model. Geophysical J Int 129:163–168

Nur A, Ofeogbu CO, Onuha KM (1999) Estimation of the depth to the Curie point isotherm in the upper Benue trough, Nigeria. J Min Geol 35:53–60

Nur A (2001) Spectral analysis and Hilbert transformation of gravity data over the southwest of the Chad Basin, Nigeria. J Min Geol 37(2):153–161

Nwankwo CN, Ekine AS, Nwosu LI (2009) Estimation of the heat flow variation in the Chad basin, Nigeria. J Appl Sci Environ Manage 13:73–80

Nwankwo LI, Olasehinde PI, Akoshile CO (2008) Spectral analysis of aeromagnetic anomalies of northern Nupe basin, west central Nigeria. Global J P Appl Sci 14(2):247–252

Nwankwo LI, Shehu AT (2015) Evaluation of Curie-point depths, geothermal gradients and near-surface heat flow from high-resolution aeromagnetic (HRAM) data of the entire Sokoto Basin. J Volcanol Geother Res 30(5):45–55

Nwankwo LI (2015) Estimation of depths to the bottom of magnetic sources and ensuing geothermal parameters from aeromagnetic data of Upper Sokoto Basin. Nigeria Geothermics 54:76–81. doi:10.1016/j.geothermics.2014.12.001

Nwankwo LI, Olasehinde PI, Akoshile CO (2011) A new technique for estimation of upper limit of digitization spacing of aeromagnetic maps. Nigerian J Physics 22(1):74–79

Obaje NG (2009) Geology and resources of Nigeria, lecture notes in earth sciences, 120, Springer-Verlag, Berlin Heidelberg

Odebode MO (2010) A handout on geology of boron (Chad) basin. Nigeria, Northeastern

Okubo YRG, Graff RO, Hansen K, Ogawa H, Tsu F (1985) Curie point depths of the Island of Kyushu and surrounding areas. Geophysics 53:481–494

Olugbemiro RO, Ligouis B, Abaa SI (1997) The Cretaceous Series in the Chad Basin, NE Nigeria: source rock potential and thermal maturity. J Min Geol 20(1):51–68

Osazuwa IB, Ajakaiye DE, Verheijen PJT (1981) Analysis of the structure of part of the Upper Benue Rif Valley on the basis of new geophysical data. Earth Evol Sci 2:126–133

Ravat D, Pignatelli A, Nicolosi I, Chiappini M (2007) A study of spectral methods of estimating the depth to the bottom of magnetic sources from near-surface magnetic anomaly data. Geophys J Int 169:421–434

Ross HE, Blakely RJ, Zoback MD (2006) Testing the use of aeromagnetic data for the determination of Curie depth in California. Geophysics 71(5):L51–L59

Saada SA (2016) Curie point depth and heat flow from spectral analysis of aeromagnetic data over the northern part of Western Desert, Egypt. J Appl Geophys 134:100–111

Salk M, Pamukcu O, Kaftan I (2005) Determination of the Curie point depth and heat flow from Magsat data of Western Anatolia. J Balk Geophy Soc 8(4):149–160

Shuey RT, Schellinger DK, Tripp AC, Alley LB (1977) Curie depth determination from aeromagnetic spectra. Geophys J R Astron Soc 50:75–101

Spector A, Grant FS (1970) Statistical models for interpreting aeromagnetic data. Geophysics 35:293–302

Tanaka AY, Okubo Y, Matsubayashi O (1999) Curie point depth based on spectrum analysis of the magnetic anomaly data in East and Southeast Asia. Tectonophysics 306:461–470

Thebault E, Purucker M, Kathryn A, Langlais WB, Sabaka TJ (2010) The magnetic field of the earth's lithosphere. Space Sci Rev 155:95–127

Wright JB (1976) Volcanic rocks in Nigeria. In: Kogbe CA (ed) Geology of Nigeria, 2nd edn. Rock View International, France

Wright JB, Hastings D, Jones WB, Williams HR (1985) Geology and mineral resources of West Africa. George Allen and Urwin London 90–120